

## Supplementary Information

### **Memory, switches, and logic gates through bistability in chemically fueled crystals**

Fabian Schnitter<sup>1</sup>, Benedikt Rieß<sup>1</sup>, Job Boekhoven<sup>1,2,\*</sup>

1 Department of Chemistry, Technical University of Munich, Lichtenbergstrasse 4, 85748 Garching, Germany.

2 Institute for Advanced Study, Technical University of Munich, Lichtenbergstrasse 2a, 85748 Garching, Germany.

\*Correspondence to: [job.boekhoven@tum.de](mailto:job.boekhoven@tum.de)

## Supplementary methods

### Turbidity measurements

The evolution of the turbidity during the reaction cycle is measured with an Arduino controlled setup (Supplementary Figure 5). The setup measures the scattering of 660 nm laser light under a 90° angle. The main advantage of such a setup compared to a commercial setup is the possibility to continuously stir the sample and connect it to inflow and outflow tubing. The scattering rate is measured at 10-second intervals. By using a smaller stirring plate, the setup can be put into an incubation chamber to control the temperature during the reaction cycle. The Arduino script is provided at: <https://github.com/fabianschnitter/Script-turbidity-device.git>.

### Steady state experiments.

We used a continuously stirred tank reactor to create steady state concentrations. The reactor setup was made up of a 1.5 ml HPLC vial equipped with a micro stir bar put on a stir plate (600 rpm). The reactor was continuously supplied by a  $0.3 \text{ mL}\cdot\text{min}^{-1}$  inflow from a 150 mM precursor **1** or **3** stock solution ( $0.12 \text{ mL}\cdot\text{min}^{-1}$  from a 37.5 mM precursor **2** stock solution). The inflow rate of EDC was equal to the inflow rate of precursor, but the stock concentration varied to apply different molar fluxes. The outflow rate was  $0.6 \text{ mL}\cdot\text{min}^{-1}$  ( $0.24 \text{ mL}\cdot\text{min}^{-1}$  for precursor **2**). Aladdin AL-1000 syringe pumps from WPI were used equipped with 20 ml Braun Injekt syringes (ID = 20.10 mm). We used silicone tubing (OD = 1.8 mm, ID = 1.0 mm) and Braun Sterican needles (ID = 0.8 x 120 mm) for injection. For the outflow, a tygon tubing (OD = 3.2 mm, ID = 1.6 mm) was directly placed through a pre sliced septum of the HPLC vial in the reactor. A tubing diameter of 1.6 mm appeared to be best to homogeneously remove the solution with the crystals. At lower diameters, the tubing tended to clog, whereas larger diameters reduce the velocity which is necessary to remove the crystals. We tested the quality of constantly removing the crystal state anhydride by measuring the sum of concentration acid and anhydride inside the reaction vessel over time to exclude up concentration of the precursor (see Supplementary Figure 4). For longer experiments larger 50 ml Braun Omnifix syringes (ID = 27.90 mm) were used. To measure the turbidity of the sample, the HPLC vial was placed in the home-made turbidity device. The temperature was controlled by placing the entire setup in an incubator. Measuring the reaction mixture's temperature was done by the In-outdoor Traceable thermometer purchased from VWR. The reaction vessel was supplied by the syringe pumps placed outside the incubator at controlled 21 °C ambient temperature. We prevented the reaction mixture to cool down by placing roughly 20 cm of tubing inside the incubator to allow the influx solution to approach the set incubator's temperature (see Supplementary Figure 4). As a starting reaction mixture, 100 mM precursor **1**, 10 mM precursor **2**, or 150 mM precursor **3** was used. Thereby, addition of the 80 mM EDC spike (50 mM regarding **2**) before

pumping resulted in initial crystal or droplet formation. To measure the reaction cycle's concentrations, 30  $\mu$ l aliquots were taken over time and quenched with a 200 mM benzylamine solution (1:1 dilution).

### **Determining the temperature dependence of $S_{out}$ and $S_{sat}$ .**

The  $S_{out}$  and  $S_{sat}$  was determined in steady state experiments, spiking the system beforehand applying a 10 mM. $\text{min}^{-1}$  EDC and 30 mM. $\text{min}^{-1}$  precursor **1** flux. This EDC flux did not sustain the crystalline on state which was shown by a decrease in scattering. We assumed a complete dissolution of the crystals at the timepoint reaching 0.15 scattering units. The anhydride concentration calculated by the kinetic model at this timepoint was taken as the  $S_{out}$ . The supersaturation concentration  $S_{sat}$  could not be measured directly as common methods like cooling down a solution of a known concentration is not possible. During the reaction cycle, anhydride is constantly produced and consumed and a change in temperature affects the steady state concentration. Furthermore, the induction time must be considered when directly measuring  $S_{sat}$ , which is the time between reaching a supersaturated solution and the onset of detectable nucleation<sup>1</sup>. Instead, we approached the supersaturation concentration by increasing the EDC flux and measuring the scattering of the system in steady state. For instance, at 21 °C, an EDC flux between 20 and 25 mM. $\text{min}^{-1}$  evoked a crystal steady state detected by an increase in scattering. The corresponding anhydride steady state concentration was calculated by the kinetic model and taken as  $S_{sat}$  in the phase diagram.

### **Toggling the switch experiments**

The reactor was loaded with 1.5 ml water. The syringes were operated for 5 min to establish steady state concentrations (21 °C, 150 mM acid **1** stock, 100 mM EDC stock, inflow 0.3 ml. $\text{min}^{-1}$ , respectively). For the activation, different amounts of EDC were added from a 2 M stock solution (30.0  $\mu$ l, 22.5  $\mu$ l, 15.0  $\mu$ l, 7.50  $\mu$ l), whereas the crystalline anhydride of **1** and the salts (NaCl: 438 mg, 263 mg, 88.0 mg; NaBr: 464 mg; NaI: 675 mg) were added as solids. As the crystalline anhydride was added in small amounts (1.6 mg, 1.1 mg, 0.54 mg, 0.11 mg), the reactor's volume was increased to 5 ml (150 mM acid stock, 100 mM EDC stock, inflow 1.0 ml. $\text{min}^{-1}$ , respectively). Polystyrene (1.5 mg) was added as a control to ensure that the change in volume did not induce crystallization.

For the deactivation, 1.5 ml of 100 mM precursor **1** solution was initially activated with 40 mM EDC. After stabilizing the reactor for 5 min by pumping (21 °C, 150 mM acid **1** stock, 100 mM EDC stock, inflow 0.3 ml. $\text{min}^{-1}$ , respectively), deactivation was done by adding various amounts of high concentrated stock solutions (5 M benzylamine: 90  $\mu$ l, 60  $\mu$ l, 45  $\mu$ l; 33 wt% methylamine: 100  $\mu$ l, 75  $\mu$ l, 50  $\mu$ l; 70 wt% ethylamine: 69  $\mu$ l, 61  $\mu$ l, 52  $\mu$ l; 5 M 3-(dimethylamino)-1-propylamine: 120  $\mu$ l, 105  $\mu$ l, 90  $\mu$ l) to the reaction vial. The dilution was kept well below 10%.

When switching the system several times, a fraction of the reaction solution was replaced by the deactivation stock to prevent volume expansion.

### **Pixel-display experiment.**

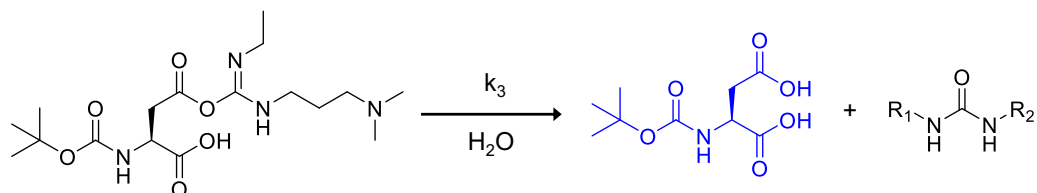
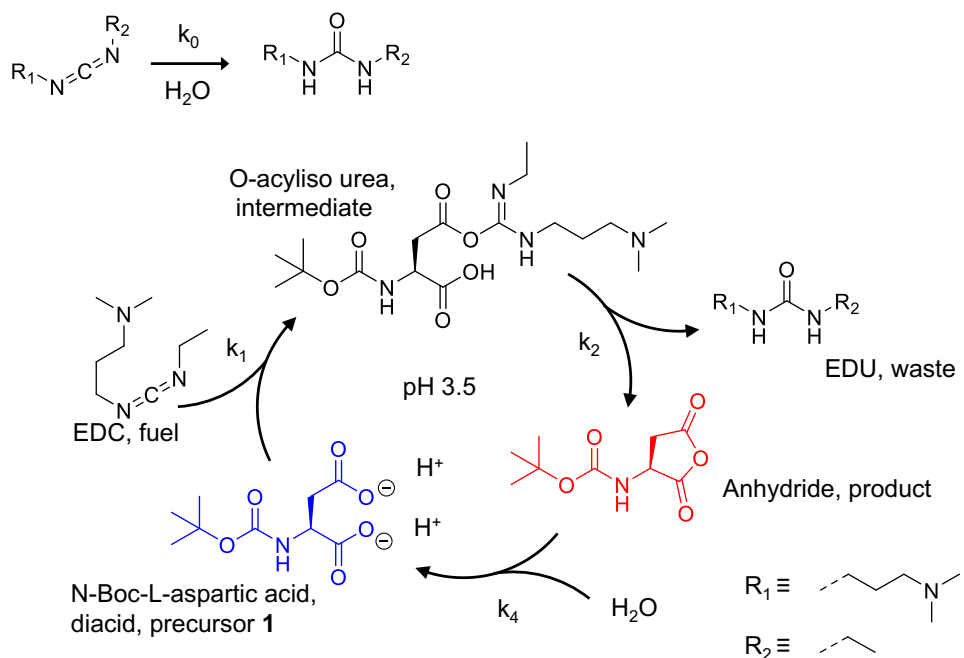
The 3x3 pixel display reactor was 3D printed using the Form 2 from Formlabs applying a black photopolymer resin. After the print, the 3x3 pixel display was treated 20 min with isopropanol and cured for 5 min at 55 °C. Each of the nine reactors was filled 0.6 mL of 100 mM precursor **1**. Then, the flowrate in was set to 0.12 ml·min<sup>-1</sup> (150 mM acid stock, 100 mM EDC stock) and the flowrate out to 0.24 ml·min<sup>-1</sup>. To control 27 syringes simultaneously, two Aladdin AL-1600 and five Aladdin AL-1000 were used with 3D printed extensions to hold three syringes instead of one (see Supplementary Fig. 19). The 3x3 pixel display was placed on a stir plate. Activation of the pixels was done by the addition of 12 µL of a 2 M EDC stock, whereas deactivation was done by replacing 36 µL of the reaction solution with 36 µL 5 M benzylamine solution. Timelapsed photographs in 10 seconds intervals were recorded by a Logitech BRIO webcam. Processing the photographs was done by imageJ extended by a fiji distribution. The 3D model 3x3 pixel display as well as the extension of the pumps can be found at: <https://www.thingiverse.com/thing:4960191> and <https://www.thingiverse.com/thing:4971601>.

### **Boolean logic gate experiment.**

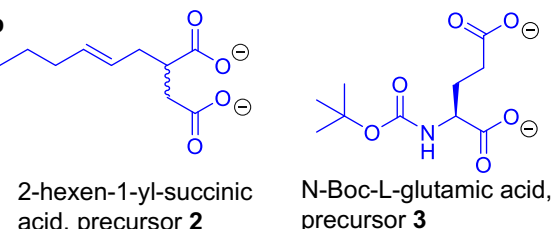
A 1x3 reactor array was 3D printed as described above. Luer lock connectors were designed to easily connect the reactors with the inflow tubing. The outflow tubing is connected via a hole at the back of the reactors. At the bottom, cuvette micro stirrers from 2MAG are placed right beyond the reaction reactors. The flow from the input to the output reactor takes place via a 2 mm diameter hole. The reactor's turbidity is monitored by time lapsed photographs of the outflow tubings in 10 seconds intervals. Each reactor was filled with 1.5 ml water. Then, each reactor received an influx of 20 mM·min<sup>-1</sup> EDC and 30 mM·min<sup>-1</sup> precursor **1**. Specifically, the input reactors received 0.3 ml·min<sup>-1</sup> of a 150 mM acid **1** stock and 0.3 ml·min<sup>-1</sup> of a 100 mM EDC stock. From the input reactors, 0.4 ml·min<sup>-1</sup> was withdrawn, and 0.2 ml·min<sup>-1</sup> flowed into the output reactor. The output reactor received 0.1 ml·min<sup>-1</sup> of a 450 mM precursor **1** stock and 0.1 ml·min<sup>-1</sup> of a 300 mM EDC stock. A more detailed overview is given in Supplementary Figure 17. Moreover, the output reactor also received 0.2 ml·min<sup>-1</sup> from each input reactor. Activation of the input reactors was done by the addition of 30 µL from a 2 M EDC stock or 263 mg NaCl. Deactivation was done by replacing 90 µL of the reaction solution with 90 µL 5 M benzylamine solution. The 3D model can be found at: <https://www.thingiverse.com/thing:4971613>.

## Supplementary Figures

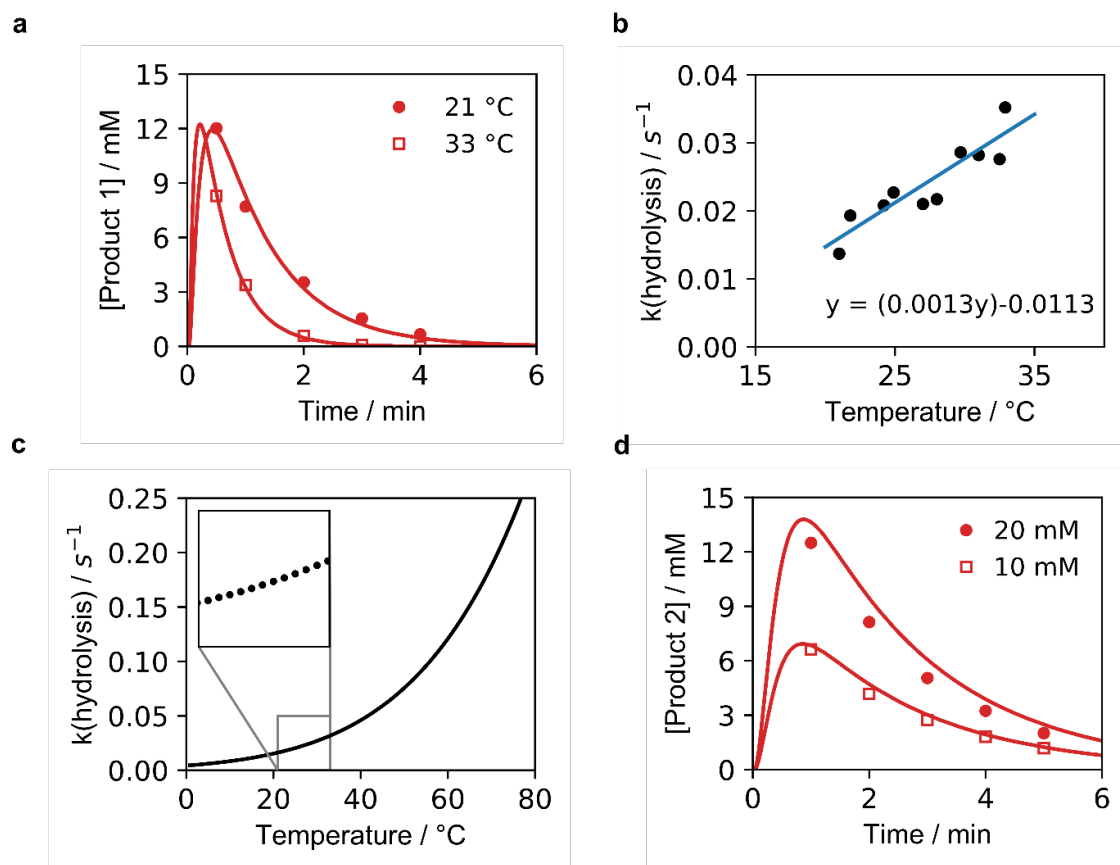
a



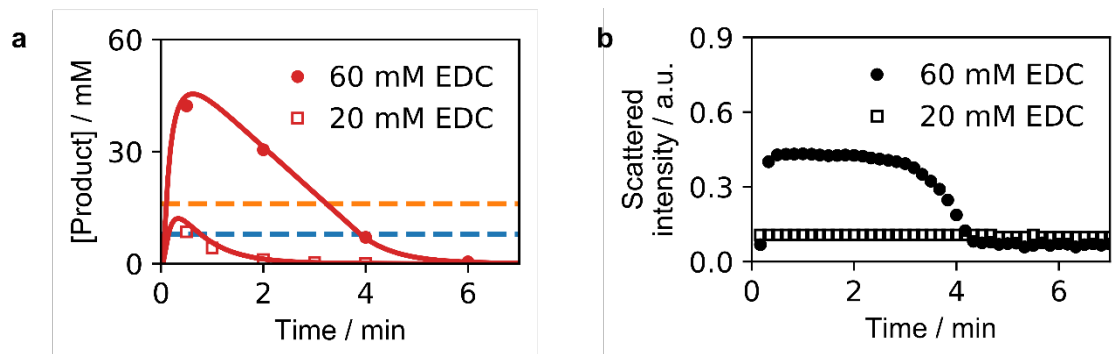
b



**Supplementary Figure 1. The reactions involved in the chemical reaction cycle. a,** All reactions shown are simultaneously taking place at various rates. The direct hydration of the EDC fuel ( $k_0$ ) was examined in previous work<sup>2</sup>. The start of the reaction cycle is the addition of one EDC molecule to the diacid precursor, forming a high energy intermediate ( $k_1$ ). On releasing the waste product EDU, the intermediate further reacts to the active anhydride product ( $k_2$ ). Furthermore, the intermediate decomposes in a side reaction at low rates to the precursor by direct hydrolysis ( $k_3$ ). The deactivation reaction comprises the degeneration of the precursor driven by the anhydride hydrolysis ( $k_4$ ). **b,** Further diacids used as precursors.

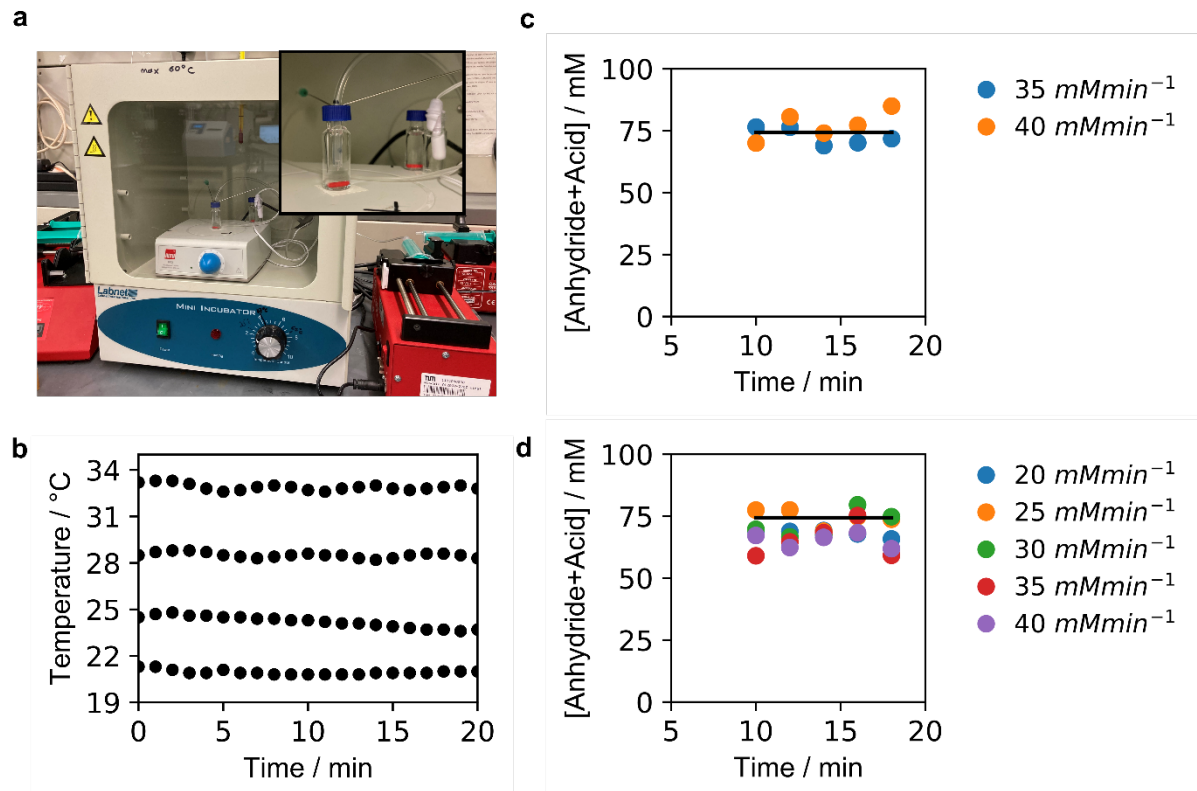


**Supplementary Figure 2. Batch fueled experiments to extract deactivation rate constants.** **a**, The first order decay profile of anhydride product **1** hydrolysis over time at various temperatures. The profiles at 21 °C and 33 °C are taken as exemplary curves for all temperatures measured. **b**, The deactivation rate constants of **1** determined for different temperatures. **c**, The effect of temperature on  $k_4$  of **1** as calculated by the Arrhenius correlation. **d**, The first order decay profile of **2** when fueling with different amounts of EDC.

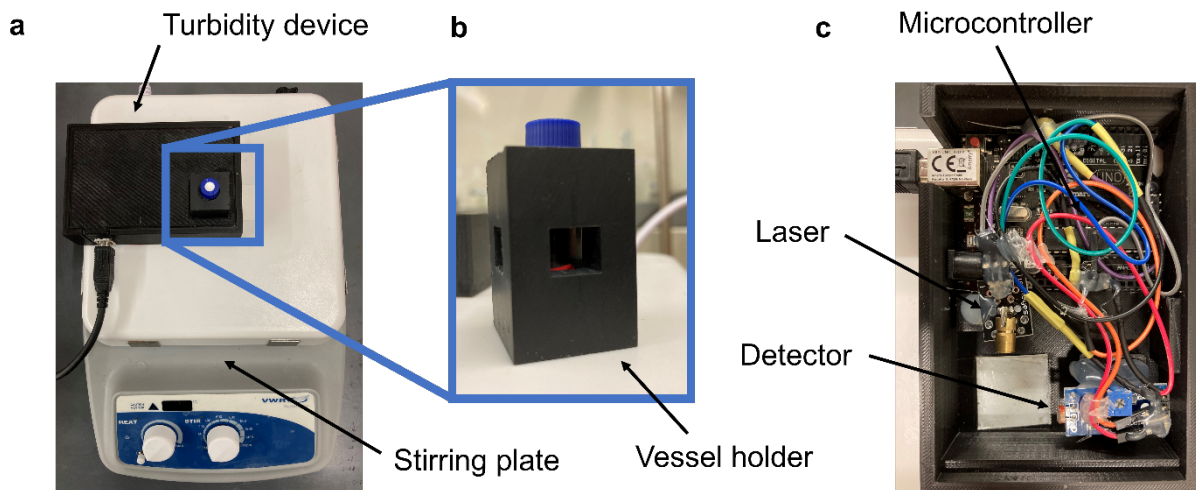


**Supplementary Figure 3. The reaction cycle's response at 24 °C when adding different amounts of EDC fuel to 100 mM precursor **1**.** **a**, When adding 20 mM of EDC, the anhydride yield is below  $S_{\text{sat}}$  (orange line), whereas when increasing the EDC amount to 60 mM the anhydride concentration exceeds  $S_{\text{sat}}$ . **b**, The measured scattering shows the presence of

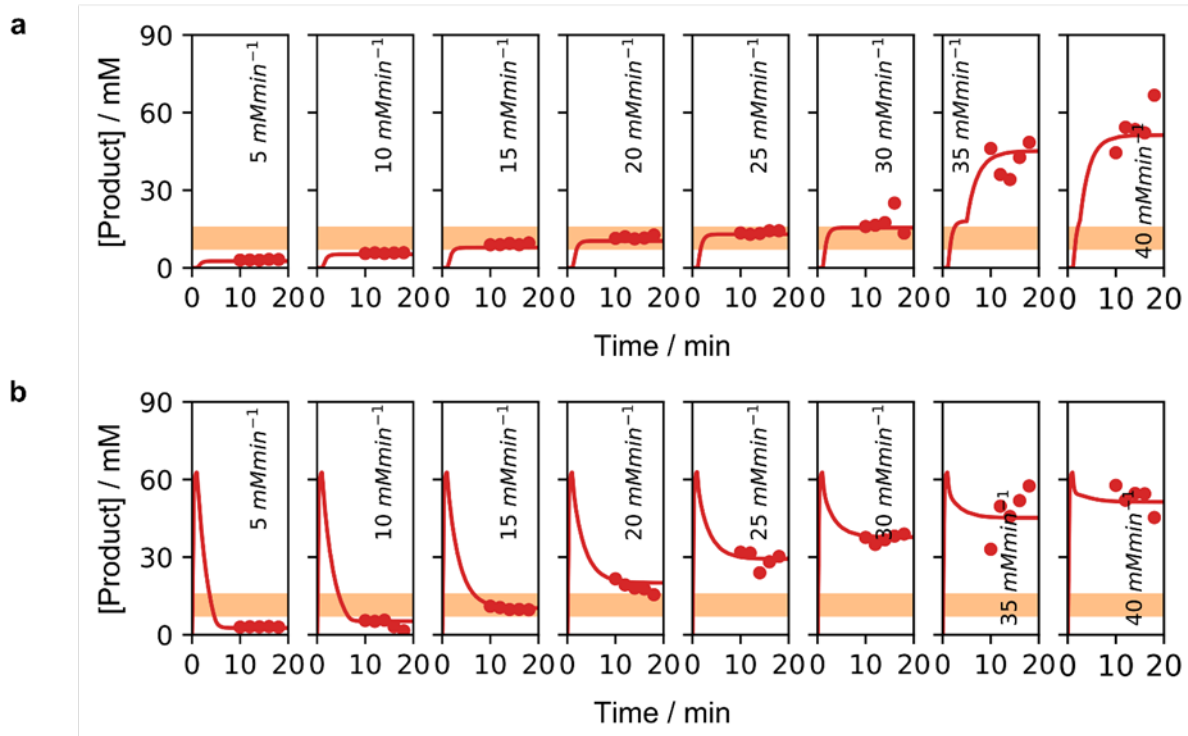
crystals when 60 mM fuel is added, whereas no increase in scattering was measured for 20 mM EDC addition.



**Supplementary Figure 4. Experimental setup of steady state experiments.** **a**, Photograph of the experimental setup. **b**, Monitoring the temperature stability of the steady state experiments. **c, d**, The sum of the concentration precursor **1** and the corresponding product over time. The concentration should be roughly and ensures that the crystals are not clogging the tubing, or accumulate in the reactor. In the date in **c**, no spike was added. In contrast, an 80 mM EDC spike was added at **d**. The markers represent HPLC data, and the line represents the concentration predicted by the kinetic model.

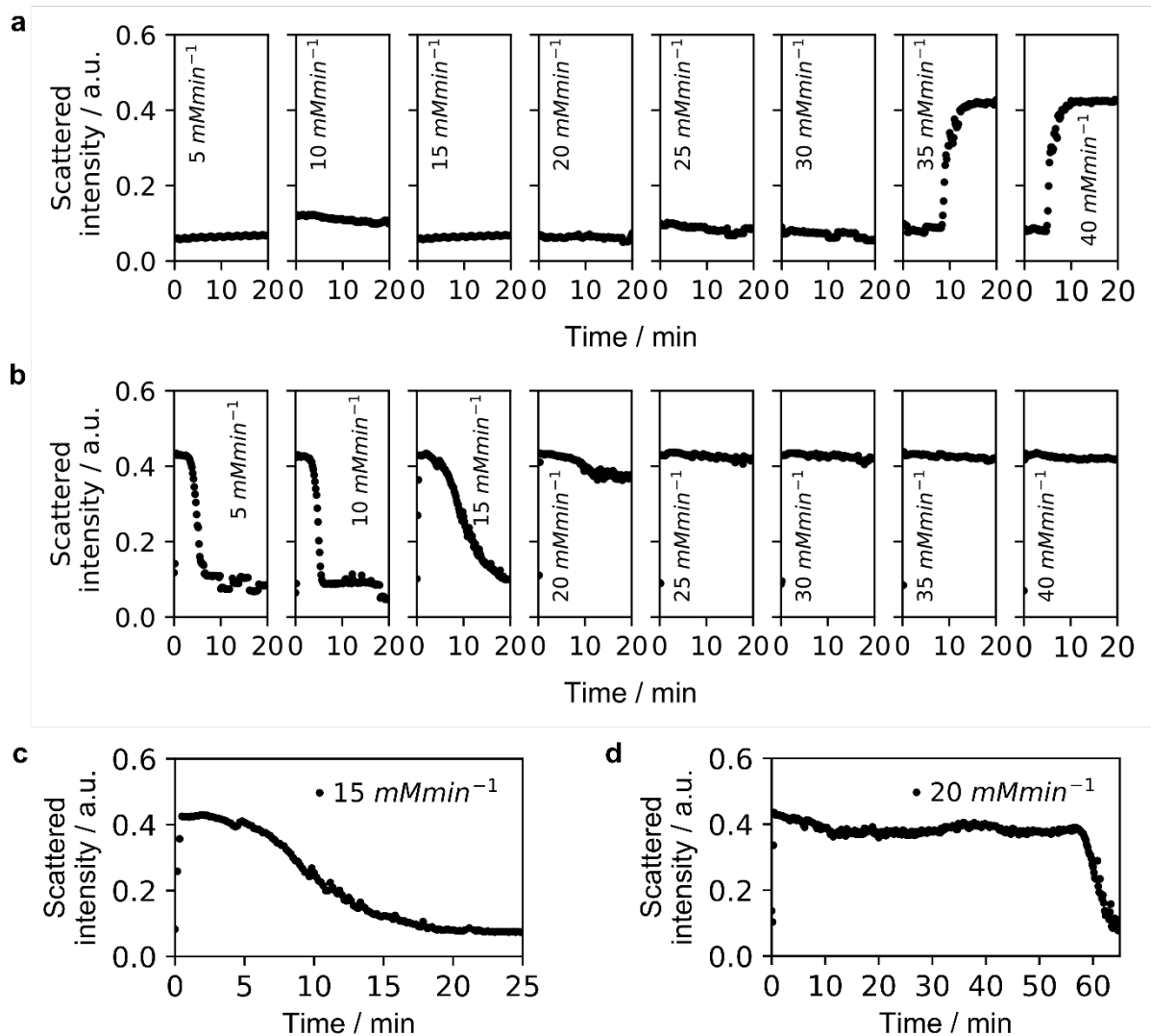


**Supplementary Figure 5. The setup used to measure the reaction cycle's turbidity.** **a**, The device is placed on a stirring plate to homogeneously mix the crystals formed by the anhydride. **b**, An HPLC vial was used as sample container, which is placed inside a 3D printed vessel holder. **c**, The scattered light is measured under a 90° angle. The laser and detector are controlled by an Arduino microcontroller. The electronic components are covered by a 3D printed case, small enough to put into an incubator on top of a small stir plate.

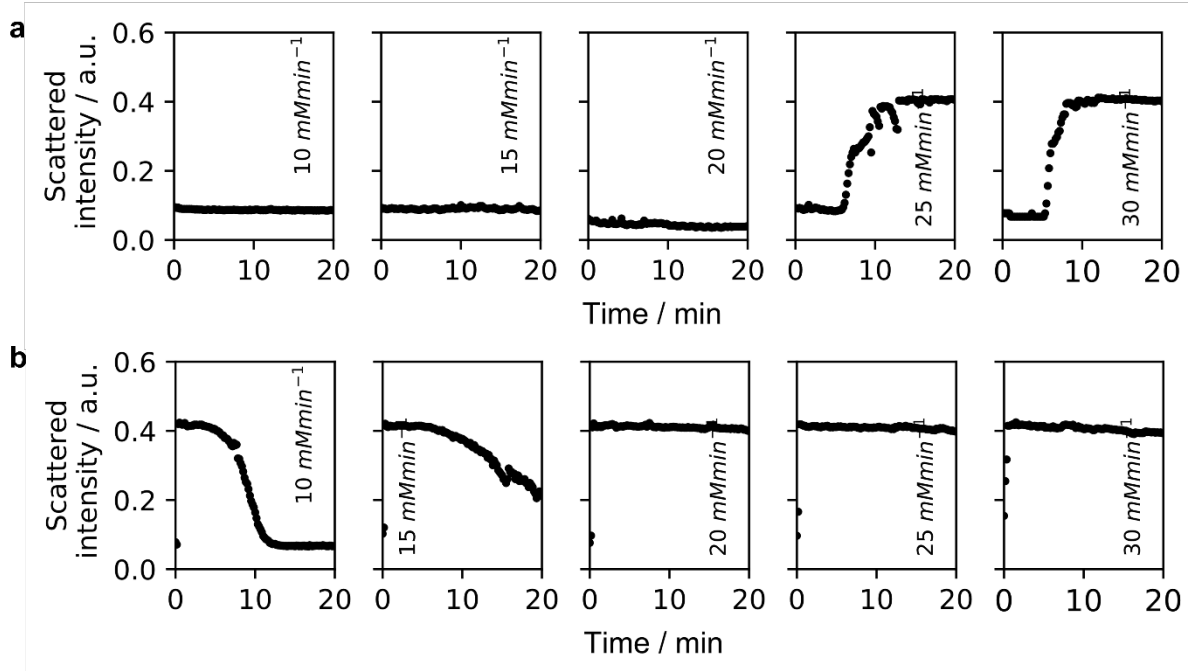


**Supplementary Figure 6. The steady state concentration of the anhydride product of 1 at 24 °C and a space velocity of 0.4 min<sup>-1</sup>.** The markers indicate concentrations measured by HPLC and the solid line represents modelled data. **a**, When fueling at least with 35 mM·min<sup>-1</sup> EDC, the steady state concentration surpasses the metastable zone (marked orange) and crystal formation starts resulting in much higher steady state levels. **b**, When adding an 80 mM

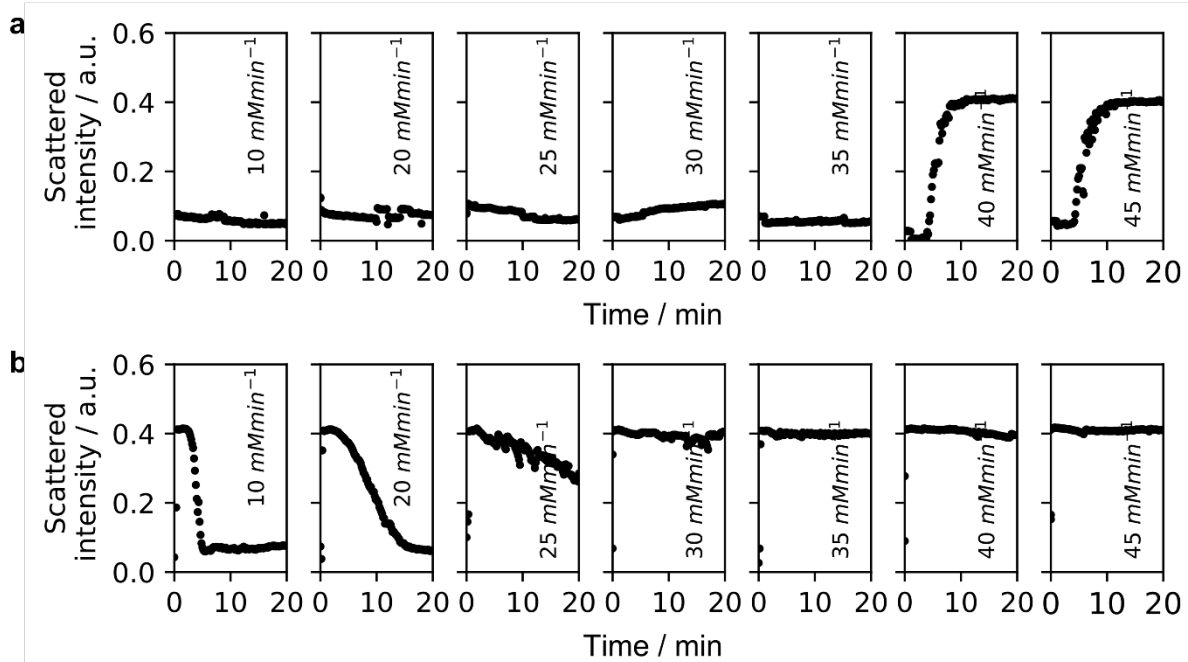
EDC spike before starting the constant influx of EDC and precursor, crystal formation already starts at lower fuel influxes, i.e., at  $20 \text{ mM} \cdot \text{min}^{-1}$  EDC.



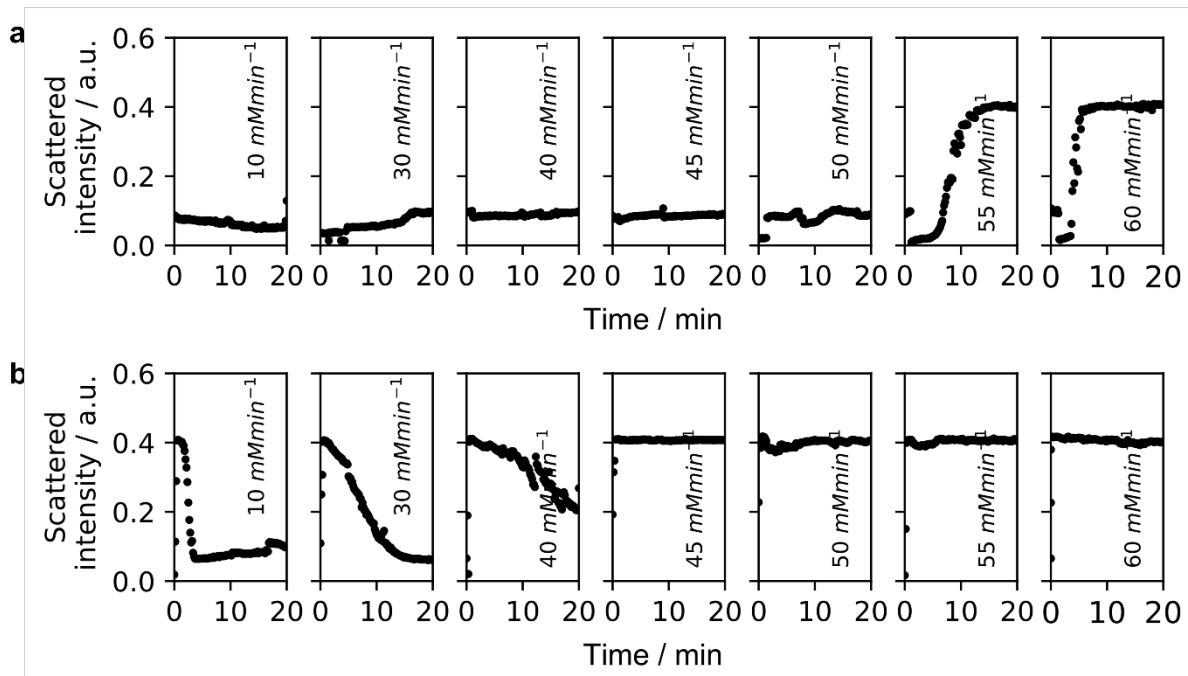
**Supplementary Figure 7. The scattering of reaction cycle 1 as a measure for turbidity at 24 °C and a space velocity of 0.4 min<sup>-1</sup>.** **a**, When applying at least a 35 mM·min<sup>-1</sup> EDC flux, crystallization starts to occur which is shown by an increase in the scattering at 10 min. **b**, The addition of an 80 mM EDC spike before starting the influx of EDC and precursor results in initial crystal formation. Low EDC fluxes are not sufficient to sustain the crystals. At a 20 mM·min<sup>-1</sup> EDC flux, a steady state in turbidity could be reached at around 10 min which indicates the persistent presence of crystals. **c, d**, The curves from b measured for longer times.



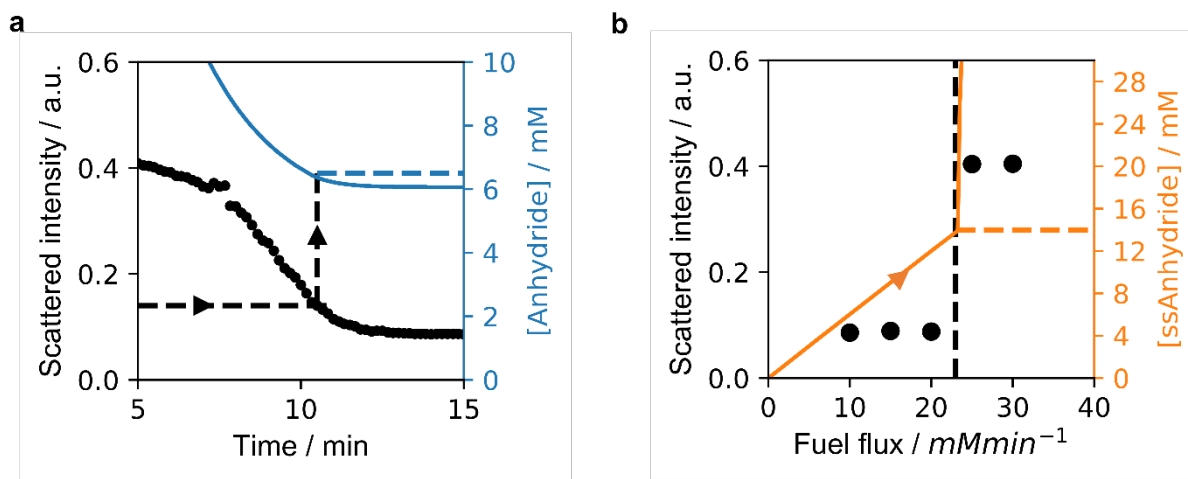
**Supplementary Figure 8.** The scattering of reaction cycle 1 as a measure for turbidity at 21 °C and a space velocity of 0.4 min<sup>-1</sup>. **a**, No EDC and **b**, an 80 mM EDC spike was added before starting the pumps.



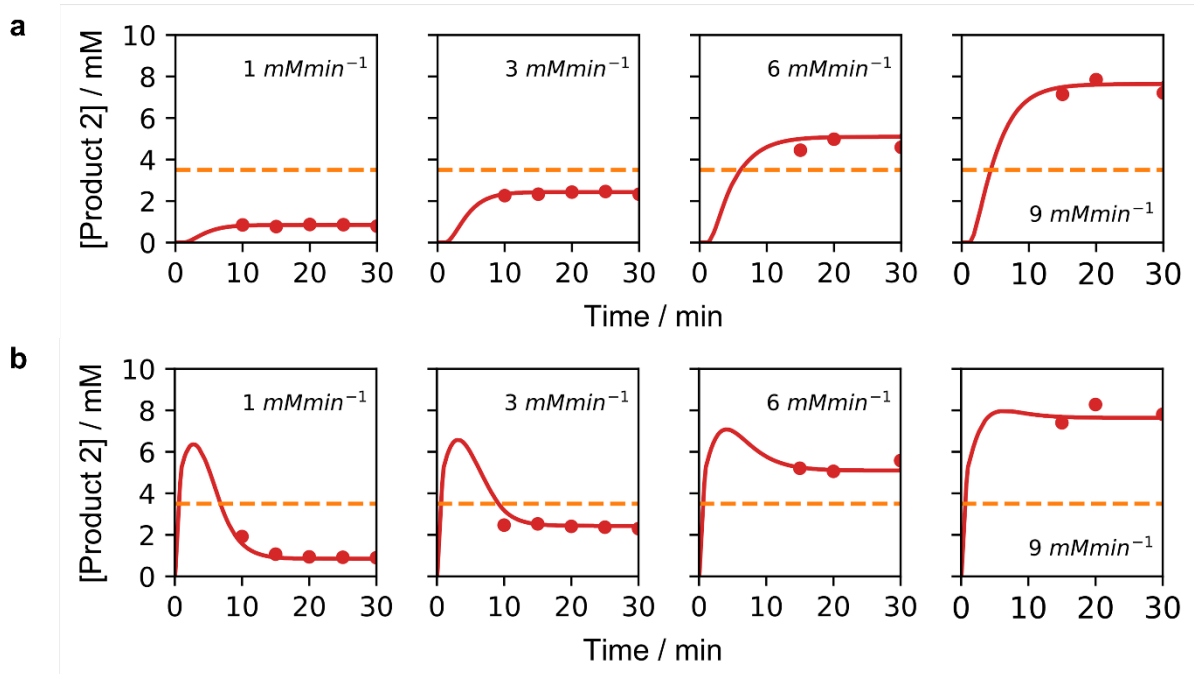
**Supplementary Figure 9.** The scattering of reaction cycle 1 as a measure for turbidity at 28 °C and a space velocity of 0.4 min<sup>-1</sup>. **a**, No EDC and **b**, an 80 mM EDC spike was added before starting the pumps.



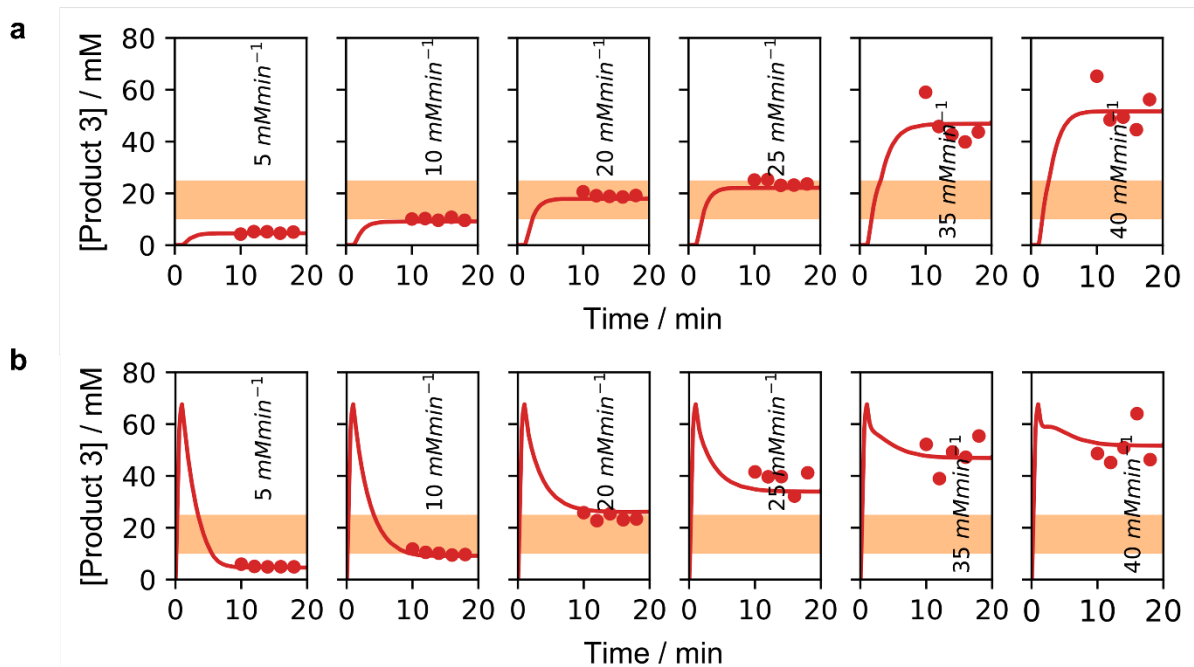
**Supplementary Figure 10. The scattering of reaction cycle 1 as a measure for turbidity at 33 °C and a space velocity of 0.4 min<sup>-1</sup>.** **a**, No EDC and **b**, an 80 mM EDC spike was added before starting the pumps.



**Supplementary Figure 11. Determining the temperature dependence of  $S_{out}$  and  $S_{sat}$ .** The procedure is exemplary shown at 21 °C for all temperatures in the phase diagram. **a**, The scattering over time when a 10 mM·min<sup>-1</sup> EDC flux was applied to the reaction vessel after adding an 80 mM EDC spike at 21 °C. The blue line represents the anhydride evolution over time calculated by the kinetic model and yields  $S_{out}$ . **b**, The steady state scattering measured when different EDC fluxes are applied at 21 °C. The orange line represents the appearing steady state concentration in anhydride calculated by the model and yields  $S_{sat}$ .

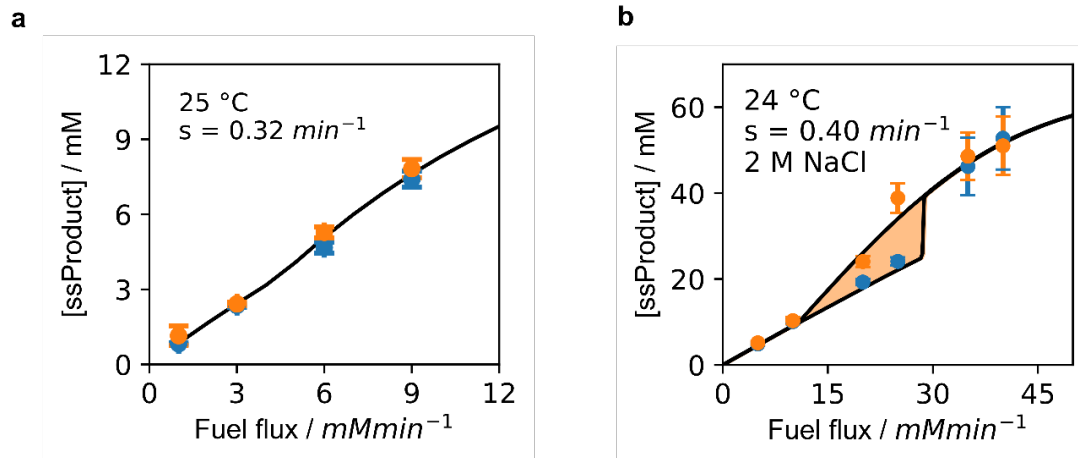


**Supplementary Figure 12.** The steady state concentration of the anhydride product of 2 at 25 °C, pH 6.0 and a space velocity of 0.32 min<sup>-1</sup>. The markers indicate concentrations measured by HPLC and the solid line represents modelled data. Whilst the precursor influx was kept constant at 6 mM·min<sup>-1</sup>, several EDC fluxes were applied when **a**, no EDC and **b**, a 50 mM EDC spike was added at the beginning.

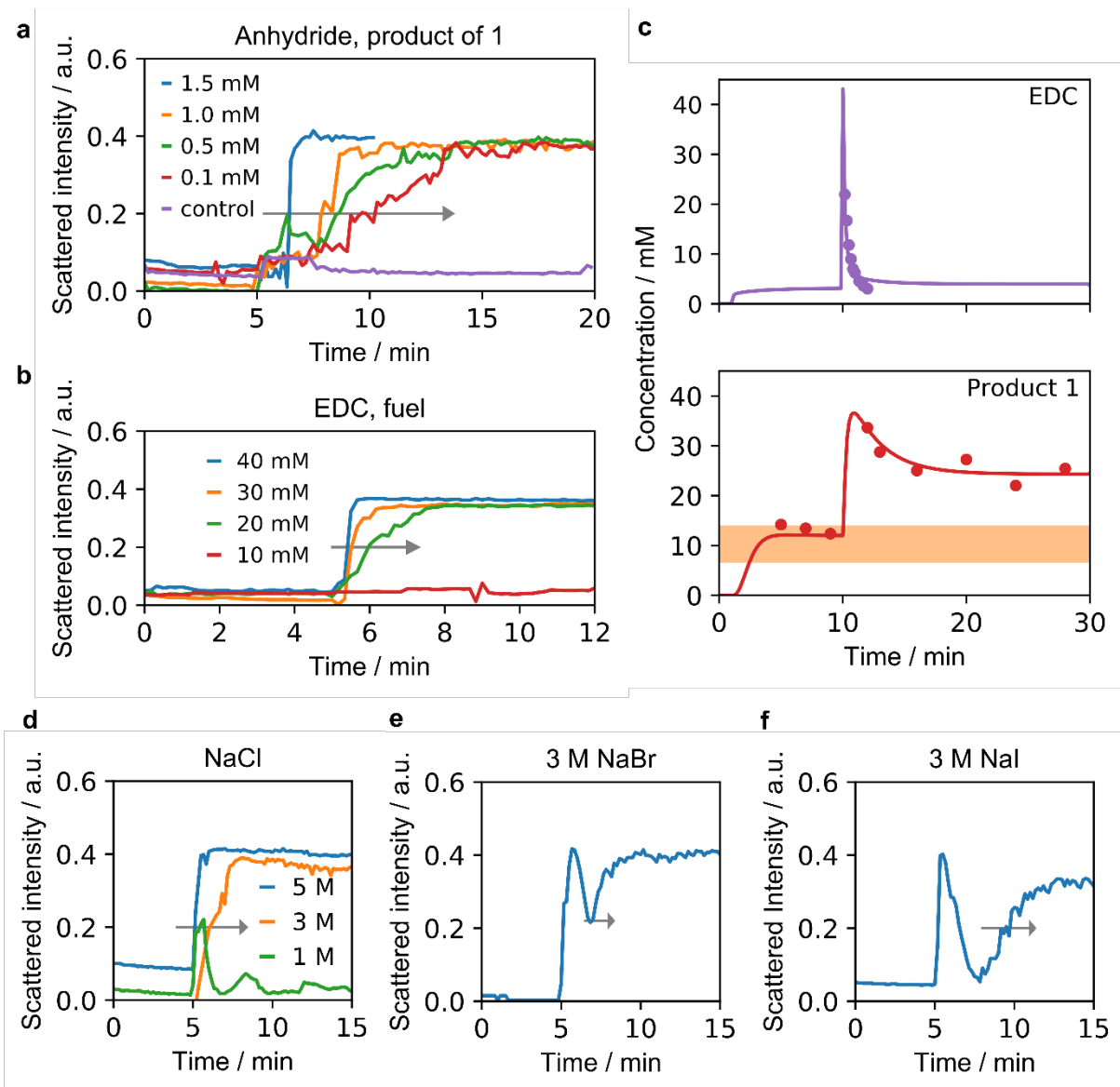


**Supplementary Figure 13.** The steady state concentration of the anhydride product of 3 at 24 °C, pH 3.5 and a space velocity of 0.4 min<sup>-1</sup>. The markers indicate concentrations measured by HPLC and the solid line represents modelled data. The precursor was influxed

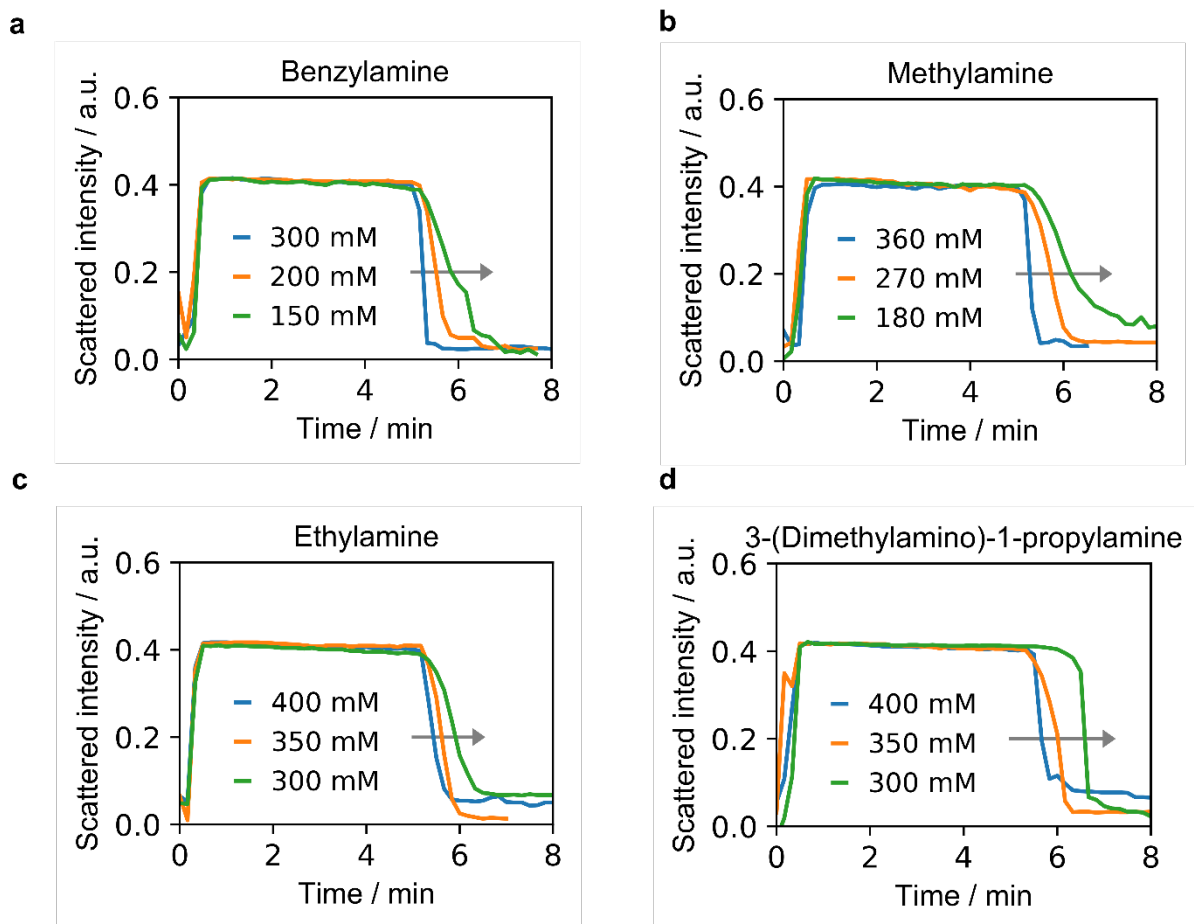
continuously at a rate of  $30 \text{ mM} \cdot \text{min}^{-1}$ . Increasing the EDC flux increases the steady state concentration and **a**, crystals start to form at an EDC flux of at least  $35 \text{ mM} \cdot \text{min}^{-1}$ . **b**, When adding an  $80 \text{ mM}$  EDC spike before starting the pumps, an EDC flux of  $20 \text{ mM} \cdot \text{min}^{-1}$  is sufficient to form sustained crystals and results in higher anhydride steady state concentrations.



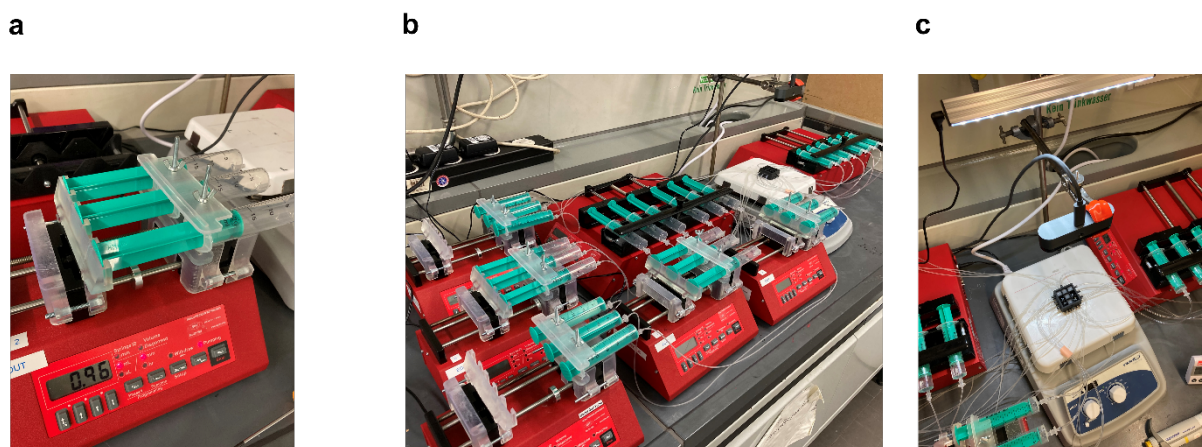
**Supplementary Figure 14. Hysteresis curves of further precursors.** The markers represent the measured mean steady state concentration of **a**, precursor **2** and **b**, precursor **3** and their standard deviation ( $n=5$ ). The line is calculated by the kinetic model.



**Supplementary Figure 15. Toggling the switch experiment - Activation.** Various triggers were applied to switch the system on at 5 min when influxing  $20 \text{ mM} \cdot \text{min}^{-1}$  EDC and  $30 \text{ mM} \cdot \text{min}^{-1}$  precursor **1** at  $21^\circ\text{C}$ . The scattering over time taken as a measure for turbidity when **a**, seeding with crystalline anhydride. As a negative control, polystyrene beads were added to test the effect of additional nucleation sites. **b**, The effect upon turbidity when adding various fuel concentrations and **c**, the steady state concentrations of EDC and anhydride over time. The transient addition of 40 mM EDC switches a steady state concentration inside the metastable zone to a higher steady state concentration with sustained crystal formation. **d**, The effect of adding high concentration crystalline NaCl, **e**, NaBr and **f**, NaI.

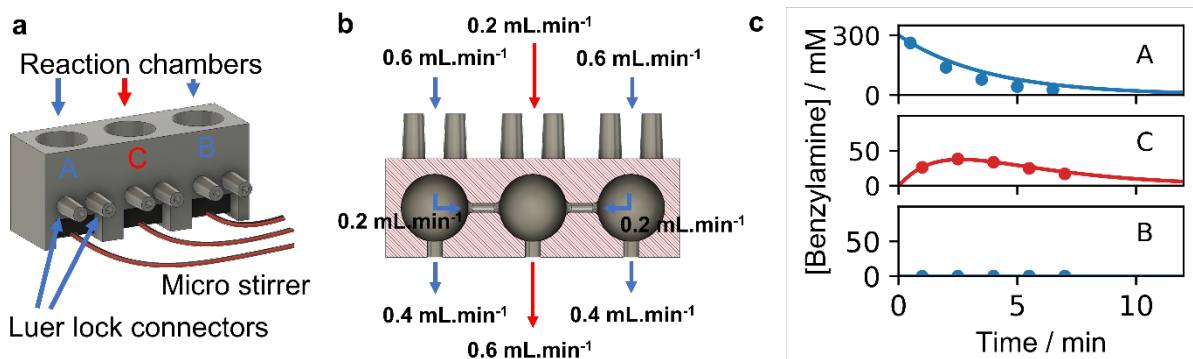


**Supplementary Figure 16. Toggling the switch experiment - Deactivation.** The system was influxed with  $20 \text{ mM} \cdot \text{min}^{-1}$  EDC and  $30 \text{ mM} \cdot \text{min}^{-1}$  precursor 1. Spiking with  $40 \text{ mM}$  EDC before starting the pumps led to a sustained on state. At 5 min (a) benzylamine, (b) methylamine, (c) ethylamine (d) a propylamine derivative was added as an off trigger. The decrease in scattering was measured over time to estimate the effectiveness of deactivation.

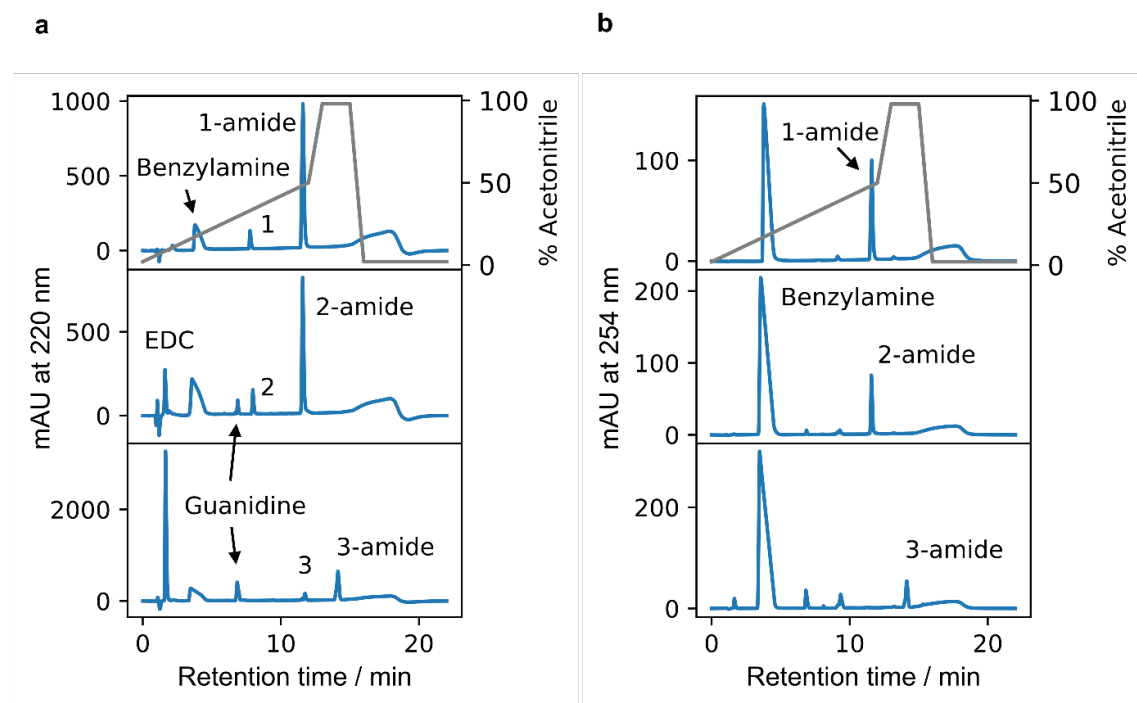


**Supplementary Figure 17. The experimental setup of writing pixel-based patterns.** **a**, The 3D printed extension allows to control three syringes with one syringe pump. **b**, To influx and

outflux one reactor, three syringes are needed giving a total number of 27 syringes for a 9-digit pixel display. **c**, The 3x3 array was placed on a stir plate and timelapse photographs were taken by a webcam.



**Supplementary Figure 18. A 3D printed setup to combine three switches to an OR logic gate.** **a**, The reactors A and B correspond to the input reactor and the middle reactor C serves as a readout. Each reactor is individually fueled with precursor **1** and EDC under a constant outflux. **b**, A connection between the reactors allows an influx from the outer reactors into the middle reactor. **c**, The influx of reactor A to C is tested by adding 300 mM of benzylamine to reactor A and monitoring the concentration over time by HPLC (marker). The line is predicted by the Matlab model.



**Supplementary Figure 19. The HPLC chromatograms of the quenched reaction cycle.** Retention times and pump gradient of cycle **1**, **2** and **3** as recorded at **a**, 220 nm and **b**, 254 nm.

## Supplementary Tables

|  | precursor 1                    |                     |                     |                     | precursor 2           | precursor 3 <sup>3</sup> |
|--|--------------------------------|---------------------|---------------------|---------------------|-----------------------|--------------------------|
|  | 21 °C                          | 24 °C               | 28 °C               | 33 °C               | 24 °C                 | 25 °C                    |
| $k_1$ (M <sup>-1</sup> s <sup>-1</sup> ) | 0.500                          |                     |                     |                     | 0.450                 | 0.200                    |
| $k_2$ (s <sup>-1</sup> )                 | 0.600*k <sub>1</sub>           | 1.14*k <sub>1</sub> | 1.20*k <sub>1</sub> | 1.60*k <sub>1</sub> | 0.150*k <sub>1</sub>  | 1.00*k <sub>1</sub>      |
| $k_3$ (s <sup>-1</sup> )                 | 0.0500*k <sub>1</sub>          |                     |                     |                     | 0.0100*k <sub>1</sub> | 0.250*k <sub>1</sub>     |
| $k_4$ (s <sup>-1</sup> )                 | (0.00130*Temperature) – 0.0113 |                     |                     |                     | 0.00740               | 0.00350                  |

**Supplementary Table 1: The rate constants used in the kinetic model.**

## References for Supplement

1. Kulkarni, S.A., Kadam, S.S., Meekes, H., Stankiewicz, A.I. & ter Horst, J.H. Crystal Nucleation Kinetics from Induction Times and Metastable Zone Widths. *Crystal Growth & Design* **13**, 2435-2440 (2013).
2. Tena-Solsona, M. et al. Non-equilibrium dissipative supramolecular materials with a tunable lifetime. *Nat Commun* **8**, 15895 (2017).
3. Wanzke, C., Tena-Solsona, M., Rieß, B., Tebcharani, L. & Boekhoven, J. Active droplets in a hydrogel release drugs with a constant and tunable rate. *Materials Horizons* **7**, 1397-1403 (2020).